Geometry of turbulence in wall-bounded shear flows: periodic orbits

P. Cvitanović and J. F. Gibson

School of Physics, Georgia Institute of Technology, Atlanta, GA 30332, USA

Abstract. The dynamical theory of moderate Reynolds number turbulence triangulates the infinite-dimensional Navier-Stokes state space by sets of exact solutions (equilibria, relative equilibria, periodic orbits, ...) which form a rigid backbone which enables us to describe and predict the sinuous motions of a turbulent fluid. We report determination of a set of unstable periodic orbits from close recurrences of the turbulent flow. A few equilibria that closely resemble frequently observed but unstable coherent structures are used to construct a low-dimensional state-space projection from the extremely high-dimensional data sets. The turbulent flow can then be visualized as a sequence of close passages to unstable periodic orbits, i.e, time-recurrent dynamical coherent structures typical of the turbulent flow.

PACS numbers: 05.45.-a, 47.10.ad, 47.10.Fg, 47.11.-j, 47.27.-i, 47.27.De, 47.27.ed, 47.27.ek, 47.27.N-, 47.27.nd

Submitted to: *Phys. Scr.*

1. Introduction

In the world of everyday, moderately turbulent fluids flowing across planes and through pipes, advances in observation and computation are changing the ways we think about hydrodynamic flows. The dynamical (as opposed to statistical) theory of moderate Re turbulence in wall-bounded flows is making significant progress. Recent experiments are very impressive, with the resolution of $3D$ particle-image velocimetry (PIV) measurements of turbulent pipe flows almost comparable to the numerical simulations. There is a multitude of new exact numerical solutions that one dared not dream about a decade ago, and portraits of turbulent fluid's state space geometry are unexpectedly elegant. The theory triangulates the infinite-dimensional Navier-Stokes state space (not low-dimensional models) by sets of exact solutions (equilibria, traveling waves, periodic orbits, ...) which form a rigid backbone that enables us to describe and predict the sinuous motions [1] of a turbulent fluid exemplified by figure 1.

The time evolution of such flows is profitably visualized in the state space, as described below in section 3. Such state space visualizations promise to be a useful tool for viewing both experimental data and numerical simulations. The idea is to pick a few typical coherent structures observed in a turbulent flow PIV data or simulation, and use these to construct a low-dimensional state-space projection from the extremely high-dimensional data set. Evolution of a typical turbulent flow is then visualized in terms of close passages to the unstable coherent structures observed in turbulent regions of the state space.

Here we give a brief overview of the recent progress on this front. Sections 2 and 3 summarize the technical preliminaries described in detail in refs. [2, 3, 4]. Section 4 introduces the new, previously unpublished periodic orbits results. Writing about turbulence is a bit like writing about ballet without seeing any. The reader might enjoy viewing the three kinds of accompanying animations on ChaosBook.org/tutorials [5]:

(i) $3D$ movies of velocity fields turbulent flows visiting unstable coherent structures

(ii) State-space trajectories, which show that (a) recurrent coherent structures arise from close passes to unstable equilibrium and periodic orbit solutions of Navier-Stokes, and (b) that these invariant solutions and their unstable manifolds impart a rigid structure to state space that organizes the turbulent dynamics.

(iii) The dual views show some of these animations side-by-side. In these, one sees recurrent coherent structures appear in the turbulent velocity field as the state-space trajectory makes close passes to invariant solutions of Navier-Stokes.

In what follows, the key ideas are illustrated in the context of plane Couette flow. Similar phenomena have been observed in pipe flows [6, 7, 8, 9]. Many people (see the acknowledgements below) have contributed to this effort. Here we cite only a few articles that cover technical aspects of results discussed here; for an overview of the literature, see ref. [2].

2. $3D$ visualization of plane Couette flow

An instant in the evolution of plane Couette flow in a rectangular cell of size $[L_x, L_y, L_z] = [15, 2, 15]$ is shown in figure 1. In all simulations presented here the Reynolds number based on half the wall separation and half the relative wall speed is $Re = 400$. At this Re, sufficiently large perturbations of the laminar flow become turbulent, and the turbulent flow settles into similar patterns of behavior in which counter-rotating streamwise rolls and associated streaks of high and low-speed fluid predominate, with the rolls spanning the distance between the two walls. It is striking that these same recognizable unstable but recurrent structures appear in a wide range of simulations and experimental conditions. But what, exactly, are these structures, and how can they be identified and related? These questions motivate all that follows, both the numerical searches for unstable invariant solutions, and their state space visualization.

Figure 1 shows a flow in a cell large enough to mimic experimental conditions [10, 11]. The walls are in principle infinite in extent, but the size of observed structures is

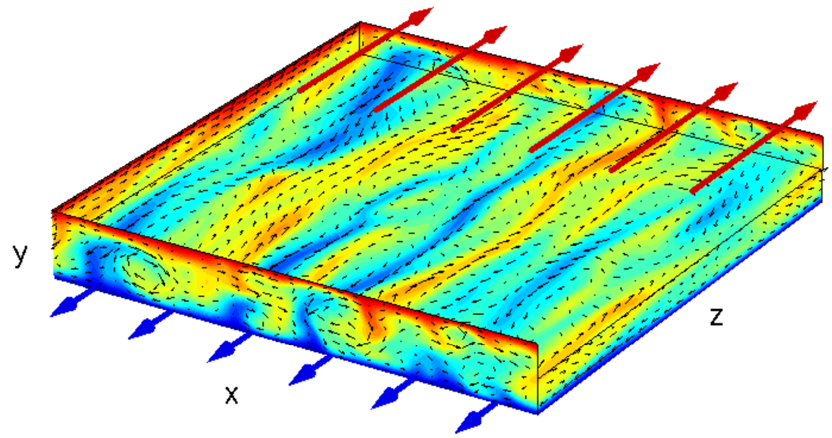

Figure 1. (color online). Plane Couette flow in a large aspect ratio periodic cell. The $[x, y, z]$ directions are referred to as streamwise, wall-normal and spanwise, respectively, velocity components are denoted by $\boldsymbol{u}(\boldsymbol{x}, t) = [u, v, w](x, y, z, t)$. The grayscale (color) indicates $u(\boldsymbol{x}, t)$, the streamwise speed of the fluid: light (red) indicates fluid being dragged away from the viewer by the top wall, dark (blue) towards, and arrows indicate fluid velocity in the section plane. The velocity field is shown in three planes: (a) the midplane $(x, 0, z)$, halfway between the upper and lower walls, (b) the $(x, y, 0)$ streamwise cross-section, in the front and top half of the back, and (c) the $(0, y, z)$ sides, top left and bottom right.

comparable to the wall-wall separation. Hence rather small aspect ratio cells (spanwise, streamwise periodic) such as those of figure 2 (a), which are simpler to analyze than figure 1, can capture the essential physics and exhibit behavior qualitatively similar to large aspect cells. Empirical searches for the smallest aspect cells still sufficiently large to exhibit (numerically) stationary turbulence were first undertaken by Hamilton, Kim and Waleffe [12]. All calculations reported here were performed for either the Ω_{HKW} or the Ω_{GHC} small aspect cells (as defined in ref. [2]).

2.1. Exact solutions of Navier-Stokes: Equilibria

The classic laminar equilibrium (steady state) has a linear profile $\boldsymbol{u} = u(y, 0, 0)$. Figure 2 (a) shows EQ_2, the Nagata [13] "upper branch," the first non-trivial, numerically exact equilibrium, found in 1990. In the past four years many new equilibria have been found [2, 3, 14]. Close passes of turbulent flow to these equilibria are evident in the movies that the reader can view on ChaosBook.org/tutorials [5] website.

The exact numerical equilibrium solutions of Navier-Stokes are pretty amazing: they are highly convoluted configurations, with the velocity field varying all over the fluid cell in a manner indistinguishable to the naked eye from snapshots of a turbulent fluid, but these solutions are stationary - they do not change under Navier-Stokes evolution, at least not until numerical errors creep in. They are robust and persist for ranges of *Re* and spanwise and streamwise wavenumbers (inverse cell sizes). The Nagata "lower-branch", the least dissipative equilibrium, has been tracked [15] for *Re* as high as 10,000. For a fixed *Re* solutions have preferred wavenumbers fixed by the interplay of the cell dimensions and the boundary layer "wall units," in ways not well understood.

Now that we have many exact solutions of Navier-Stokes equations: how do we visualize them, fit them together?

3. State space visualization: a stroll through 61,506 dimensions

In order to better visualize the relations amongst the equilibria and periodic orbits, and their relation to a typical turbulent trajectory, we have developed a new state-space visualization of moderately turbulent flows [2]. The idea is simple, but the key ingredients -exact solutions, their stability eigenvalues and eigenvectors- were not available until recently.

Think of a $3D$ state of the fluid at a given instant -the $3D$ velocity field at every point of the cell- as a point in a *state space*. In principle this space is infinite-dimensional; in practice it is always approximated by a finite-dimensional computer discretization. This dimension is bounded from below by computational accuracy needs and the cleverness of numerical algorithms. Solutions presented here are resolved to single precision accuracy, and for this cell size and Reynolds number, $61,506 \approx 10^5$ coupled ODEs turn out to be sufficient [2]. This is the number of independent variables in a $32 \times 35 \times 32$ spectral expansion of an incompressible, no-slip velocity field; larger cells and higher *Re* require more. As our exact invariant solutions require that 10^5 or more dimensions for numerical accuracy, truncated models do not capture small scales that are essential part of turbulent dynamics. We do no modeling here - all our calculations are fully resolved direct numerical simulations (DNS), carried out in the full state space.

If our visual cortex can pick out and recognize large structures in these flows, not all of these 61,506 dimensions can be equally important. Can we construct a state space coordinate system in which a few coordinates reveal the organization of the flow around these structures? We find Proper Orthogonal Decomposition (POD) helpful in identifying important directions in state space, and we are indebted to the earlier POD work [16, 17] for the idea of projecting onto characteristic states using an energy-based inner product. The kinetic energy of the fluid endows the vectors in state space (velocity field across the entire cell at a given instant in time) with a physically motivated bilinear $L2$ norm, a velocity vector dot product averaged over the cell volume:

$$E(t) = |\boldsymbol{u}|^2 = (\boldsymbol{u}, \boldsymbol{u}) \,, \quad (\boldsymbol{u}, \boldsymbol{v}) = \frac{1}{V} \int_\Omega dV \; \boldsymbol{u} \cdot \boldsymbol{v} \,. \tag{1}$$

POD is a method for construction of orthogonal coordinate frames by fitting long-time trajectory averages by ellipsoidal cigars. In contrast, the triangulation of state space by exact invariant solutions and their stable/unstable manifolds undertaken here *involves no averages* over the turbulent flow, and does not replace the true dynamics with a

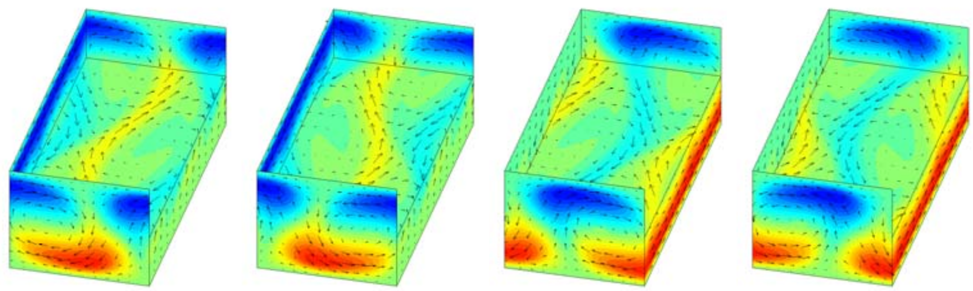

(a)

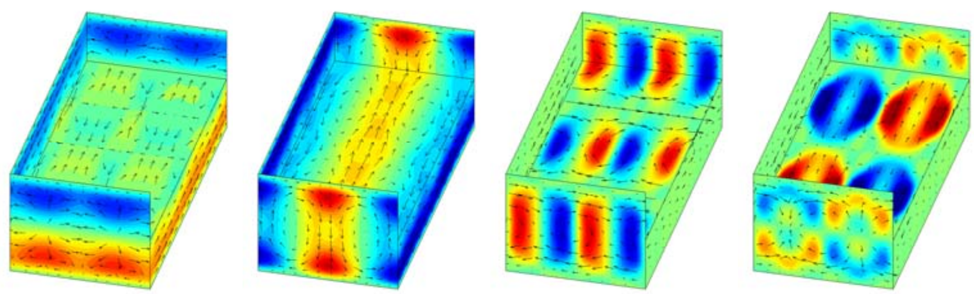

(b)

Figure 2. (color online). (a) The Nagata EQ_2 equilibrium solution and its three 1/2-cell translates. (b) The orthonormal basis set $\{\boldsymbol{e}_1, \boldsymbol{e}_2, \boldsymbol{e}_3, \boldsymbol{e}_4\}$ within the "61,506-dimensional" vector space of fluid states is constructed by adding the four Nagata solutions in symmetrized / antisymmetrized combinations. Here we plot differences from the laminar flow, otherwise, the plotting conventions are the same as figure 1.

low-dimensional model. Instead, we use exact solutions of Navier-Stokes to identify important structures and show how they organize the state space dynamics.

THE IDEA: pick a few fluid states frequently visited by the turbulent flow, and visualize the infinite-dimensional flow by projecting it onto coordinate frames constructed from these states. For wall-bounded shear flows close to the onset of turbulence such state space portraits are surprisingly informative. What are good choices of such coordinate frames? A simple choice is to form a set of basis vectors by orthogonalization of a set of physically important equilibrium solutions. For small aspect ratio cells at moderate *Re* and simple symmetry groups we are lucky: a single equilibrium and its three 1/2-cell translates, shown in figure 2 (a) produces a very nice global visualization of the dynamics. (The choice of 1/2-cell translations is related to symmetry group of the Nagata solution; for a more detailed explanation see ref. [2].) From these, we form a set of four orthonormal basis functions $\{\boldsymbol{e}_1, \boldsymbol{e}_2, \boldsymbol{e}_3, \boldsymbol{e}_4\}$, shown in figure 2 (b), and project a state-space trajectory

$$a(t) = (a_1, a_2, a_3, a_4)(t)\,, \qquad a_n(t) = (\boldsymbol{u}(t), \boldsymbol{e}_n)\,. \tag{2}$$

This produces a projection of the fully-resolved Navier-Stokes flow in 10^5 dimensions onto a four-dimensional subspace of physically important coordinates.

Figure 3 shows the state-space projection of the flow from the 10^5-dimensional space of independent variables in the numerical simulation onto the $3d$ coordinate frame

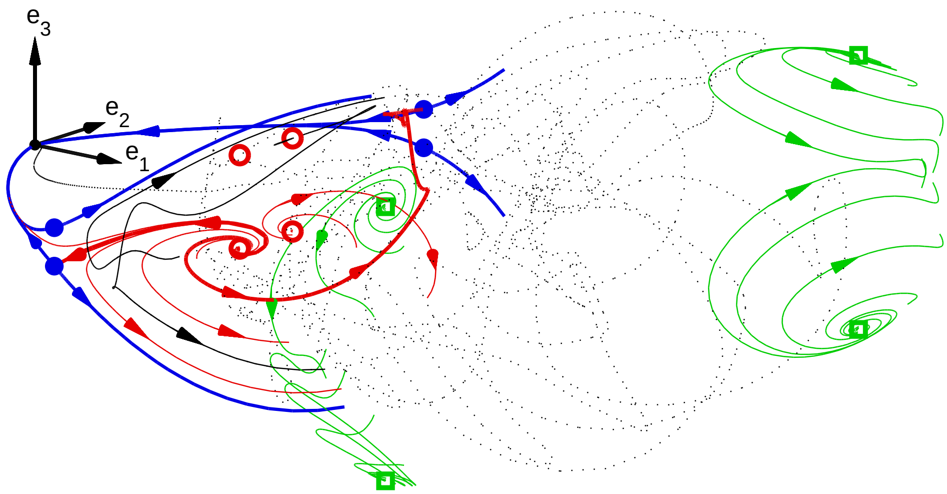

Figure 3. (color online). The state-space projection from the 10^5-dimensional space of free variables in the numerical simulation algorithm onto a $3d$ perspective projection, $\{\boldsymbol{e}_1, \boldsymbol{e}_2, \boldsymbol{e}_3\}$ basis figure 2 (b), formed from linear combinations of the Nagata upper-branch equilibrium EQ_2 and its half-cell translations, with the laminar equilibrium as the origin. Indicated are several equilibria (circles, dots, and squares), their unstable manifolds (lines emanating from symbols), and a typical turbulent trajectory (dotted). Two heteroclinic connections are shown as thick (red) lines spiralling out of one equilibrium and landing in others.

$\{\boldsymbol{e}_1, \boldsymbol{e}_2, \boldsymbol{e}_3\}$. This global portrait shows several equilibria of plane Couette flow, together with segments of their unstable manifolds traced by evolving the velocity field under Navier-Stokes. The dense dotted region indicates the natural measure generated by typical long-lived turbulent transients. Evidently the set of invariant solutions provides a "cage" that confines and organizes the turbulent flow (for details see refs. [2, 3, 4]).

This visualization is *physical*, independent of whether the $\boldsymbol{u}(\boldsymbol{x}, t)$ data is fetched from a numerical simulation or an experiment. The global portrait *is not static*, it is a picture comprised of thousands of videos: Each curve in figure 3 traces out a single state space trajectory, i.e., it corresponds to a video of a given $3D$ flow evolving in time. It is worth emphasizing that such low-dimensional projections are only a visualization, *not a reduction* of Navier-Stokes to a low-dimensional model. We do not seek a smaller set of 'modes' to represent the fluid dynamics; all calculations have to be done in high-dimensional state-spaces, with the fully resolved DNS.

Dual views of state space / 3D physical space dynamics show the plane Couette velocity field evolving under Navier-Stokes, side by side with the corresponding state-space at the same instant in time. Here we are, wandering in 61,506 dimensions. Can one slice up this high-dimensional state space into subregions, develop symbolic dynamics that assigns a precise name to each distinct exact time-invariant solution of Navier-Stokes equations?

One possible path is suggested by the existence of heteroclinic connections between

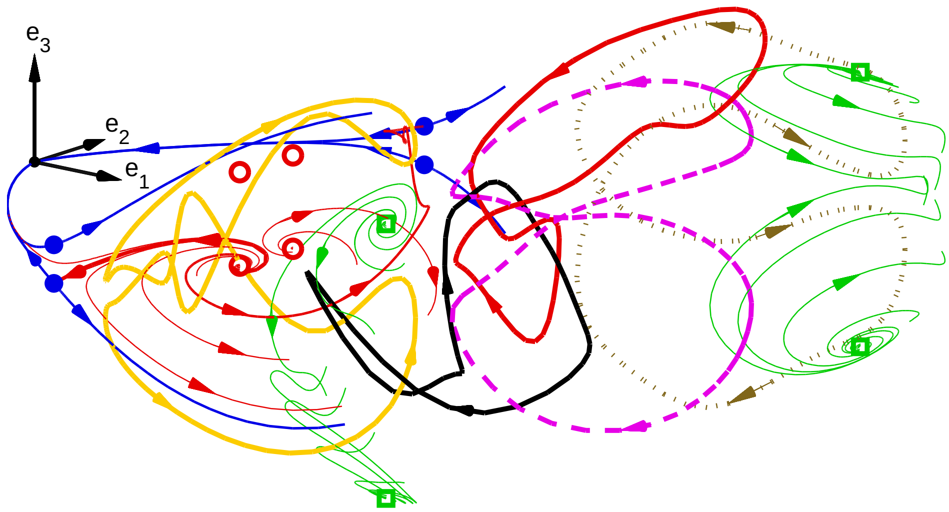

Figure 4. (color online). Five periodic orbits in the state-space projection. The orbits have symmetric counterparts that appear as mirror images in $\boldsymbol{e}_2$ and $\boldsymbol{e}_3$; these are not shown. Note that the orbits are embedded in the natural measure (dotted line in figure 3) of the turbulent flow and thus capture its dynamics and statistics. These orbits are the beginning of an infinite hierarchy of unstable periodic orbits embedded in the turbulent flow. From their $3D$ videos it would be hard to tell that these are not segments of a turbulent orbit - they capture well the typical coherent structures observed in turbulent flows.

different unstable solutions [4]. Each heteroclinic connection is traced out by an infinite-time state space trajectory, i.e., it corresponds to one $3D$ flow evolving in time. The reader is urged to explore ChaosBook.org/tutorials [5] for a dual-view movie of evolution along several heteroclinic connections. Dual visualization helps develop intuition about how states of different arrangements of rolls and streaks transmogrify into each other, and coarsely partition state space into regions tied to each other by topologically robust heteroclinic connections.

4. Turbulence and its periodic-orbit shadows

Equilibria, their stable/unstable manifolds and their heteroclinic connections teach us a lot about the geometry of the state space, but equilibria are steady states of the Navier-Stokes flow. But, by definition, they do not move, so no turbulence takes place there. To describe turbulence we need to look further, for invariant solutions that capture time-dependent dynamics. The ChaosBook.org/tutorials dual-view movies of periodic orbits and transient turbulence show that the time dependence of typical unstable structures seen in turbulence is better captured by unstable periodic orbits embedded in the turbulent regions of the state space.

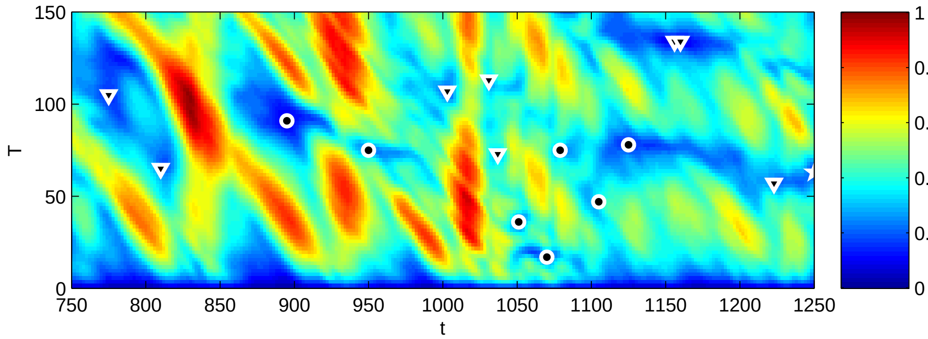

Figure 5. (color online). Time-delay plot the distance between the trajectory at the time t and the time $t + T$ later (symmetry-reduced). Dark (blue) regions correspond to close recurrences. Circles indicate initial guesses for Newton-Krylov searches that successfully converged onto periodic orbit solutions; triangles, failures.

4.1. Exact solutions: Periodic orbits

The nontrivial equilibrium solutions are pretty cool. The next set of exact solutions is more amazing still: the Eulerian velocity is time dependent, and their movies are indistinguishable from the turbulent ones, but they return *exactly* to the initial state after a given period. Several periodic orbits are plotted in figure 4. Turbulent dynamics is captured by the (infinity of) such unstable periodic solutions, each a $3D$ movie that repeats exactly after its own finite time T.

In fluid dynamics periodic orbits are the really big deal. In order to compute an exact unstable periodic solution, one needs to guess the initial velocity field at 50,000-100,000 with a sufficient accuracy that the exponentially unstable state of fluid recurs nearly exactly after an (initially unknown) period. Until the first unstable periodic solutions of Navier-Stokes were computed by Kawahara & Kida [18] in 2001, this seemed utterly out of reach. As we report here, today arbitrarily many such solutions can be determined.

The movies of the periodic orbits computed by our group are quite instructive: viewing a few movies on ChaosBook.org/tutorials website (or the full database of invariant solutions of plane Couette flow on Channelflow.org/database [19]) suffices to get the idea. What is striking about the periodic solutions is how visually similar they are to the turbulent dynamics: they also capture episodes of highly ordered motion along streamwise counter-rotating rolls, interspersed by turbulent episodes.

How does one find unstable periodic orbits? The first ones were found by parameter continuations [13, 20], but that is not feasible for finding the chaotic sets of orbits arising from Smale-horseshoe stretching and folding rather than bifurcations of stable solutions. The state-space trajectories of (transient) turbulence exhibit sequences of close passes to various equilibria, as well as near recurrences to earlier states of the flow. We search for such close recurrences in order to initiate periodic orbit seaches [21]. We quantify this by plotting in a time-delay plot the energy norm distance (1) between the trajectory at a set of times t and times $t+T$ later, as in figure 5. The virtue of initiating Newton-Krylov searches [22] by close recurrences is that the guesses are weighted by the natural measure (likelihood that the turbulent flow visits a given region of the state space), and thus preferentially find orbits embedded into the turbulent regions of the state space (see, for example, figure 4). A more systematic approach amenable to automatization eliminates continuous time in favor of the discrete time Poincaré section returns (described below). A long sequence of section crossings $\{\boldsymbol{u}(t_0), \boldsymbol{u}(t_1), \cdots\}$ for a turbulent trajectory $\boldsymbol{u}(t)$ is checked for close recurrences, $|\boldsymbol{u}(t_0) - \sigma_{n-k}\boldsymbol{u}(t_{n-k})| < \epsilon$, with the symmetry σ_{n-k} ranging over the symmetry group of the flow. This approach captures both periodic and relative periodic orbits. Currently we have some 40 periodic orbit solutions, but one can find hundreds of (relative) periodic orbits this way without much further thinking.

While it is wisest not to wade into a discussion of symmetries of solutions [3] in this brief overview, one should note that the most striking physical feature of flows with continuous symmetries is the preponderance of "drifting" or "relative" solutions such as traveling waves and relative periodic orbits. The first relative periodic orbits in the full state-space of plane Couette were computed by Viswanath [23]. Currently we have some fifteen relative orbits with streamwise phase shifts, and only one with a minute spanwise shift. This reflects the physical fact that the energy is fed into the flow by streamwise shear, and sidewise motions are only a weak, secondary effect.

Once a set of periodic orbits is found, their superposition, figure 6, illustrates the sense in which periodic orbits shadow a typical "turbulent" state-space trajectory, and serve as a systematic cover of its natural measure in the state space.

4.2. Stability of exact solutions

Spatially periodic solutions are also solutions of integer multiples of the original cell, and of plane Couette flow on an infinite domain. Solutions in these larger cells are more unstable; empirically any perturbation of a periodic solution decays quickly to the sustained turbulence state. The equilibria and periodic orbits that we have found (with exception of the laminar state) are unstable and thus never seen in long-time simulations and experiments. Fortunately, for small aspect ratio cells they are not very unstable. And in fact, we do observe close passes to the least unstable equilibria in simulations. The number of unstable eigen-directions is small, of order 2 to 10, and the leading eigenvalues are nicely separated into a few positive, exponentially expanding and an infinity of negative, exponentially contracting ones.

4.3. Partitioning the state space: Poincaré sections, symbolic dynamics

Today we can determine a large number of periodic orbit and relative periodic orbit solutions of Navier-Stokes. Each can be visualized as a 3D video, but how are we to make sense of a large number of such invariant solutions, each a different 3D video? Here is an idea. Note that for "steady turbulence" the shear forcing I by the moving walls has to be balanced by the viscous dissipation D *in the mean*, but not at any

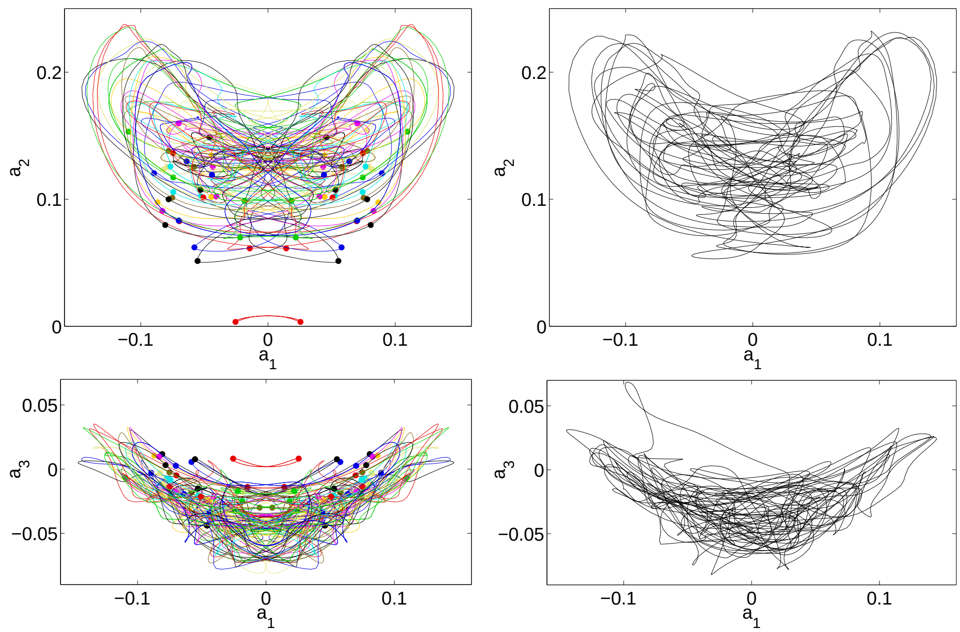

Figure 6. (color online). State-space visualization of (left) a set of periodic orbits compared to (right) the natural measure as explored by a generic turbulent trajectory. Dots on the periodic orbits indicate intersections with the $I - D = 0$ Poincaré section. The orbits are for the Ω_{HKW} cell defined in ref. [2]; the projection is onto the first three principal axes of the period $T = 87.89$ orbit together with its half-cell translation in x.

given instant in time. Let the Poincaré section H be the set of states where shear and dissipation are balanced instantaneously:

$$H = \{\boldsymbol{u} \mid h(\boldsymbol{u}) = I(\boldsymbol{u}) - D(\boldsymbol{u}) = 0\,, \quad \text{and} \quad \dot{h}(\boldsymbol{u}) < 0\}\,,$$

H is a curved hypersurface in the energy-norm based projections, since D is a nonlinear function of $\boldsymbol{u}$. This is a good Poincaré section, as (a) it is physically motivated, (b) all equilibria and traveling waves lie on it, and their unstable manifolds help partition it, (c) energy balance requires that all periodic and relative periodic orbits must pierce this section transversely at least once, and (d) it is invariant under the symmetries of the flow. We have determined the intersections with this Poincaré section for about 40 periodic orbits in the Ω_{HKW} cell (shown as dots in figure 6). The intersections of the periodic orbits with the Poincaré section are the fixed or periodic points of the Poincaré return map. The longer cycles have $n_p \approx T_p/t_{min}$ periodic points, where t_{min} is a typical shortest return time (the typical return times differ for different regions of the section).

In order to bootstrap this initial set of periodic points into a better and better symbolic dynamics, on might proceed as follows. Label periodic points $a, b, c, \cdots$. The Poincaré section can now be approximately partitioned into neighborhoods/cells $H = \cup H_a$ by a Voronoi triangulation, with a hyperplane through each shortest cord connecting pairs of neighboring periodic points.

We are not hopeful about looking at projections of unstable manifolds in this Poincaré section, or looking at I vs D plots. For the former, the dimensionalities are large (as few as four and as many as twenty unstable directions per orbit), and for the latter, we have done it and not learned much. However, the $I - D = 0$ Poincaré section could get us closer to understanding the network of transitions between the unstable periodic orbit neighborhoods, and the associated symbol sequences help us gain insights into the temporal evolution of turbulent dynamics. Here is the strategy (not as yet successfully implemented):

A periodic point maps into the next periodic point, giving a directed link of an approximate Markov diagram, connecting the two Voronoi cells. Starting in other parts of the Voronoi cell one determines links to other cells that can be reached in one Poincaré return. This yields a rough approximation to the Markov graph associated with this partition. Now use segments of the known periodic orbits that follow the same symbolic subsequence as starting guesses for multishooting Newton searches for periodic orbits one Poincaré return longer. The longer the segments used, the better the guess, due to the exponential closeness of trajectories that share the same finite symbol sequence. The result is exponentially more periodic points, exponentially finer state space partition, and a systematic hierarchy of longer and longer cycles.

4.4. How many periodic orbits is enough?

While the number of unstable periodic orbits for a chaotic system is infinite, the essential dynamics is captured by the set of shortest, "fundamental" orbits, with longer orbits acting as the exponentially decreasing corrections [24, 25]. Furthermore, the desired finite accuracy of theoretical predictions and the intrinsic noise always renders the number of required periodic orbits finite [26].

How many "fundamental" orbits are expected for the moderate *Re*, small aspect ratio plane Couette flow? As a warm-up, consider the Kuramoto-Sivashinsky flow, a one spatial dimension relative of the Navier-Stokes flow. In Kuramoto-Sivashinsky one looks at the smallest spatially periodic cell that exhibits stationary turbulence and finds [27] three equilibria and two traveling waves (after symmetry reduction). The shortest periodic orbits wind around these in various ways, so there might be $5 \times 4/2 = 10$ pairwise visitations which are fixed points in the $I - D = 0$ section, the basic blocks from which all longer periodic orbits are glued together. In plane Couette flow we have three spatial dimensions: Streamwise motions should be the most important ones, as this is how energy is fed into the flow, with the wall normal and spanwise motions playing secondary roles. So symbolic dynamics might need triplets of symbols, one for each direction. Each direction could have of order of ten important visitations of (relative) equilibrium pairs, and then the number of periodic orbits which are the shortest "building blocks" really shoots up. That almost all of the forty periodic orbits computed so far intersect the $I - D = 0$ section just once is thus not unexpected. Since the cell is of small aspect ratios, the dissipation at $Re = 400$ is strong, and the motions along the three directions are strongly correlated, the number of basic building blocks is possibly smaller than this pessimistic estimate, but forty "fundamental" orbits is certainly not a large number.

4.5. Do this at home: Channelflow.org

All computations reported here were performed with Channelflow.org public domain computational fluid dynamics software [28] on either modest workstations or, for systematic searches, a Linux cluster. Channelflow provides well-tested and easy-to-use implementations of numerical integration algorithms for plane Couette and channel flows, algorithms for computing equilibria, traveling waves, periodic orbits, their linear stability, and utilities for manipulating velocity fields and producing visualizations. The simulation software, scripts for producing movies, and data sets for all solutions discussed here can be downloaded from Channelflow.org/download [19].

5. Summary and conclusions

Recent advances in experimental measurements and numerical analysis of unstable coherent structures observed in transitional (i.e., close to the onset of) turbulence in wall-bounded shear flows give us detailed dynamical-systems insights in the nature of this type of turbulence.

Should this be called "turbulence?" The Reynolds number is low, in the transitional regime, and there is no inertial range in the Kolmogorov sense. Reynolds [1] described this dynamical regime as "sinuous motion" of a fluid. However, a wall-bounded flow explores a wide range of Re, from the laminar flow at the wall itself, through the boundary layer, to large Re, large scale motions further away from the wall. A precise dynamical description of unstable coherent structures observed close to the wall in all wall-bounded flows, qualitatively similar to exact solutions described here, is an important piece of the overall puzzle of turbulence.

While different equilibria, traveling waves, periodic orbits and relative periodic orbits are clearly physically distinct, it is hard to intuit how are they related dynamically from their spatial 3D movie visualizations. The insights of low-dimensional dynamical systems have been essential guide to the recent progress described here: The global dynamics of transitionally turbulent flows is revealed by their state-space portraiture. The new dynamical insights offer several new perspectives on this classical problem:

(i) Computation of dynamical averages such as turbulent drag, velocity correlations, etc.: In contrast to probabilistic and scaling approaches to large Re turbulence, the predictions here are in principle exact (obtained by periodic orbit theory) and transport properties are sensitive to the precise value of Re (lack of structural stability).

(ii) New approaches to nonlinear control: Now that we have a detailed picture of the invariant solutions of the flow, their linear stability eigenvectors, and their unstable manifolds, control systems using body or boundary forcing can be constructed to chaperon the fluid toward a desired state.

Still, much remains to be accomplished before the dynamicist's vision of turbulence becomes a part of an engineer's tool box. Application of periodic orbit theory lies far in the future: the effective methods for symmetry reductions, and for elaboration and refinement of symbolic partitions of state space need to be developed first. Once that is accomplished, we will have

(i) accurate predictions for measurable time-averaged observables for a given wall-bounded shear flow, such as the mean frictional drag for the plane Couette flow, turbulent mixing rates, etc.

(ii) a detailed qualitative and quantitative description of the geometry of turbulent flows, with dynamical insights into turbulent vs. laminar basins of attraction, and potential applications to non-local control of such flows.

Acknowledgments

We would like to acknowledge F. Waleffe and D. Viswanath for their generous guidance throughout the course of this research, and to J. Halcrow, J.R. Elton and D.W. Spieker for their contributions to this project. We have have learned much through discussions with D. Barkley, Y. Duguet, B. Eckhardt, M. Farge, S.C. Generalis, T. Itano, G. Kawahara, R.R. Kerswell, T.M. Schneider, L.S. Tuckerman, and L. van Veen. We are grateful to G. Robinson, Jr. for support. J.F.G. was partly supported by NSF grant DMS-0807574.

References

[1] O. Reynolds. An experimental investigation of the circumstances which determine whether the motion of water shall be direct or sinuous, and the law of resistance in parallel channels. *Proc. Roy. Soc. Lond. Ser A*, 174:935–982, 1883.

[2] J. F. Gibson, J. Halcrow, and P. Cvitanović. Visualizing the geometry of state space in plane Couette flow. *J. Fluid Mech.*, 611:107–130, 2008. `arXiv:0705.3957`.

[3] J. F. Gibson, J. Halcrow, and P. Cvitanović. Equilibrium and traveling-wave solutions of plane Couette flow. *J. Fluid Mech.*, 638:1–24, 2009. `arXiv:0808.3375`.

[4] J. Halcrow, J. F. Gibson, P. Cvitanović, and D. Viswanath. Heteroclinic connections in plane Couette flow. *J. Fluid Mech.*, 621:365–376, 2009. `arXiv:0808.1865`.

[5] J. F. Gibson and P. Cvitanović. Movies of plane Couette. Technical report, Georgia Inst. of Technology, 2010. `ChaosBook.org/tutorials`.

[6] B. Hof, C. W. H. van Doorne, J. Westerweel, F. T. M. Nieuwstadt, H. Faisst, B. Eckhardt, H. Wedin, R. R. Kerswell, and F. Waleffe. Experimental observation of nonlinear traveling waves in turbulent pipe flow. *Science*, 305:1594–1598, 2004.

[7] Casimir W. H. van Doorne. *Stereoscopic PIV on transition in pipe flow*. PhD thesis, Delft, 2004.

[8] H. Faisst and B. Eckhardt. Traveling waves in pipe flow. *Phys. Rev. Lett.*, 91:224502, 2003.

[9] R. R. Kerswell. Recent progress in understanding the transition to turbulence in a pipe. *Nonlinearity*, 18(6):R17–R44, 2005.

[10] K. H. Bech, N. Tillmark, P. H. Alfredsson, and H. I. Andersson. An investigation of turbulent plane Couette flow at low Reynolds numbers. *J. Fluid Mech.*, 286:291–325, 1995.

[11] O. Dauchot, F. Daviaud, and P. Manneville. Experimental evidence of streamwise vortices as finite amplitude solutions in transitional plane Couette flow. *Phys. Fluids*, 10:2597–2607, 1998.

[12] J. M. Hamilton, J. Kim, and F. Waleffe. Regeneration mechanisms of near-wall turbulence structures. *J. Fluid Mech.*, 287:317–348, 1995.

[13] M. Nagata. Three-dimensional finite-amplitude solutions in plane Couette flow: Bifurcation from infinity. *J. Fluid Mech.*, 217:519–527, 1990.

[14] T. Itano and S. C. Generalis. Hairpin vortex solution in planar Couette flow: A tapestry of knotted vortices. *Phys. Rev. Lett.*, 102:114501, 2009.

[15] J. Wang, J. F. Gibson, and F. Waleffe. Lower branch coherent states in shear flows: Transition and control. *Phys. Rev. Lett.*, 98(20):204501, 2007.

[16] N. Aubry, P. Holmes, J. L. Lumley, and E. Stone. The dynamics of coherent structures in the wall region of turbulent boundary layer. *J. Fluid Mech.*, 192:115–173, 1988.

[17] P. Holmes, J. L. Lumley, and G. Berkooz. *Turbulence, Coherent Structures, Dynamical Systems and Symmetry*. Cambridge Univ. Press, Cambridge, 1996.

[18] G. Kawahara and S. Kida. Periodic motion embedded in plane Couette turbulence: Regeneration cycle and burst. *J. Fluid Mech.*, 449:291–300, 2001.

[19] J. F. Gibson. Database of invariant solutions of plane Couette flow. Technical report, Georgia Inst. of Technology, 2010. `Channelflow.org/database`.

[20] F. Waleffe. Homotopy of exact coherent structures in plane shear flows. *Phys. Fluids*, 15:1517–1543, 2003.

[21] D. Auerbach, P. Cvitanović, J.-P. Eckmann, G. Gunaratne, and I. Procaccia. Exploring chaotic motion through periodic orbits. *Phys. Rev. Lett.*, 58:23, 1987.

[22] D. Viswanath. The critical layer in pipe flow at high Reynolds number. *Philosophical Transactions of the Royal Society A*, 2008.

[23] D. Viswanath. Recurrent motions within plane Couette turbulence. *J. Fluid Mech.*, 580:339–358, 2007. `arXiv:physics/0604062`.

[24] P. Cvitanović. Invariant measurement of strange sets in terms of cycles. *Phys. Rev. Lett.*, 61:2729, 1988.

[25] P. Cvitanović, R. Artuso, R. Mainieri, G. Tanner, and G. Vattay. *Chaos: Classical and Quantum*. Niels Bohr Inst., Copenhagen, 2010. `ChaosBook.org`.

[26] D. Lippolis and P. Cvitanović. How well can one resolve the state space of a chaotic map? *Phys. Rev. Lett.*, 104:014101, 2010. `arXiv:0902.4269`.

[27] P. Cvitanović, R. L. Davidchack, and E. Siminos. On the state space geometry of the Kuramoto-Sivashinsky flow in a periodic domain. *SIAM J. Appl. Dyn. Syst.*, 9:1–33, 2009. `arXiv:0709.2944`.

[28] J. F. Gibson. Channelflow: A spectral Navier-Stokes simulator in C++. Technical report, Georgia Inst. of Technology, 2010. `Channelflow.org`.